Fluorine Nuclear Magnetic Resonance Spectroscopy of "Transition State Analogue" Complexes of the D and L Enantiomers of *N*-Acetyl-*p*-fluorophenylalaninal and α-Chymotrypsin†

Dinesh O. Shah* and David G. Gorenstein

ABSTRACT: Fluorine nuclear magnetic resonance (NMR) spectra of *N*-acetyl-DL-*p*-fluorophenylalaninal in the presence of α-chymotrypsin show separate signals for the hemiacetal complex, the bound aldehyde, the free aldehyde, and the free hydrate. The hemiacetal formation was found to be pH dependent, with a maximum amount of the hemiacetal present around pH 8.0, where the α-chymotrypsin has a maximum rate of activity. Also, line widths at half-height and chemical shifts of the hemiacetal ^{19}F signal were found to be pH dependent, again with maximal effects occurring around pH 8.0. This is attributed to an increase in the exchange rate between noncovalent Michaelis complex and the covalent hemiacetal–enzyme complex. The ^{19}F signals assigned to the D and L enantiomers of the hydrate of the *N*-acetyl aldehyde–enzyme complex were also found to be pH dependent. Separate preparation of pure *N*-acetyl-D-*p*-fluorophenylalaninal as well as the L enantiomer and ^{19}F NMR study of their binding to α-chymotrypsin provided confirmation of the signals identified in the spectra of the DL racemate–enzyme complex. Only the L-aldehyde forms the tight hemiacetal complex.

Enzymes are predicted to bind transition-state structures more tightly than ground-state structures (Pauling, 1946; Wolfenden, 1972; Lienhard, 1972, 1973), and hence, a "transition-state analogue", a molecule that resembles the transition state, should have a higher affinity for the enzyme than substrate- or product-analogue structures.

Peptide aldehydes related to substrates have proven to be potent inhibitors of serine proteases (Aoyagi et al., 1969; Kondo et al., 1969; Kawamura et al., 1969; Ito et al., 1972, 1975; Thompson, 1973, 1974), and Thompson suggested that the tighter binding of the aldehydes derives from stabilization of a hemiacetal tetrahedral adduct formed between the enzyme active site serine and the aldehyde carbonyl. This hemiacetal complex is believed to resemble the transition-state structure in substrate hydrolysis and supposedly accounts for the aldehydes' tight binding to the serine proteases.

Evidence in support of the transition state analogue hemiacetal structure, however, has largely been indirect. Gorenstein et al. (1976) had, in fact, shown that simply binding of an aldehyde (cinnamaldehyde) to a serine protease (α-chymotrypsin) was not sufficient evidence of itself to warrant the conclusion of transition-state stabilization in its binding. This proton NMR[1] study of the cinnamaldehyde binding to α-chymotrypsin (Cht) gave no evidence for the putative hemiacetal–enzyme complex. Similarly, Breaux & Bender (1975) in a UV–vis spectroscopy study of substituted cinnamaldehydes binding to Cht could find no evidence in support of the transition state analogue hemiacetal structure. Lowe & Nurse [1977; see also Clark et al. (1977)] introduced an NMR double-resonance experiment that provided strong evidence in favor of the hemiacetal structure for the hydrocinnamaldehyde–Cht complex [as originally suggested by Schultz & Cheerva (1975)]. In this double-resonance experiment, the aldehydic proton of the aldehyde in the presence of Cht was cross saturated on proton irradiation in the region expected for the hemiacetal formed with the active site serine. In confirmation of Gorenstein's et al. (1976) earlier conclusion on cinnamaldehyde, no cross-saturation effects were noted with this aldehyde and Cht (Lowe & Nurse, 1977).

In a collaborative experiment, Lowe, Schultz, Gorenstein, and co-workers (Chen et al., 1979) applied proton NMR spectroscopy to the interaction of *N*-benzoyl- and *N*-acetyl-L-phenylalaninal with Cht and dehydroalaninyl-195-α-chymotrypsin. From line-width changes and cross-saturation effects, it was shown that these specific aldehyde transition-state analogues do bind as the hemiacetal to Cht. Proton NMR signals for the hemiacetal structure, however, were never directly observed and were only inferred from the selective cross-saturation experiments [see also Wyeth et al. (1980)].

However, in a proton and fluorine NMR investigation of *N*-acetyl- and *N*-benzoyl-DL-*p*-fluorophenylalaninal and *N*-acetyl-L-*p*-fluorophenylalaninal binding to Cht, Gorenstein & Shah (1982) provided the first direct observation of signals (fluorine) representing the hemiacetal structure and the noncovalent Michaelis complex. We now present additional evidence supporting the earlier ^{19}F NMR assignments.

Experimental Procedures

Materials

α-Chymotrypsin (bovine pancreatic) was purchased from Sigma Chemical Co. as a 3 times crystallized and lyophilized, salt-free type II powder. Active site titration of the enzyme followed the method of Schonbaum et al. (1961) and routinely yielded 80–85% active sites.

N-Acetyl-DL-p-fluorophenylalaninal was prepared as previously described (Gorenstein & Shah, 1982).

N-Acetyl-L-p-fluorophenylalanine. *N*-Acetyl-DL-*p*-fluorophenylalanine methyl ester (3 g, 12.55 mmol) was dissolved in methanol (21 mL) and was added to a solution of Cht (100 mg) in double-distilled water (180 mL). The pH was maintained at 7.5 ± 0.5 by the slow, manual addition of 0.2 N NaOH, and all the ester was added over a period of 45 min. The pH remained almost constant after 25 mL of 0.2 N NaOH had been added. The reaction mixture was further

† From the Department of Chemistry, University of Illinois at Chicago, Chicago, Illinois 60680. *Received June 8, 1983.* Support by the NIH (GM-17575) and the NSF for assistance in the purchase of the NMR spectrometers is acknowledged.

[1] Abbreviations: Cht, α-chymotrypsin; NMR, nuclear magnetic resonance; BzPheal, *N*-benzoylphenylalaninal; AcPheal, *N*-acetylphenylalaninal; AcFPheal, *N*-acetyl-*p*-fluorophenylalaninal; Me_2SO, dimethyl sulfoxide; EDTA, ethylenediaminetetraacetic acid.

0006-2960/83/0422-6096$01.50/0

stirred at room temperature for an additional 1 h. The aqueous solution was extracted with ethyl acetate (2 × 100 mL), and the separated aqueous phase was lyophilized to dryness. The residue (1.55 g) was dissolved in a minimum amount of water (5 mL) and precipitated by the addition of concentrated hydrochloric acid to pH 2. The separated fine white solid product was filtered under suction, washed on the filter with cold 0.01 N HCl with cooling, and dried in a vacuum desiccator over NaOH pellets; yield 0.65 g (46%); mp 140–143 °C; ^{1}H NMR (Me_2SO-d_6) δ 6.95–7.3 (m, 4 H, aromatic), 5.9–6.35 (br, 1 H, NH), 4.3–4.7 (m, 1 H, CH), 3.0–3.2 (d, 2 H, CH_2), 1.8 (s, 3 H, $NHCOCH_3$). Anal. Calcd for $C_{11}H_{12}O_3NF$: C, 58.66; H, 5.33; N, 6.22; F, 8.44. Found: C, 58.34; H, 5.51; N, 6.17; F, 8.44.

The ethyl acetate extract was washed first with 0.01 N HCl (2 × 50 mL) and then with cold water (2 × 50 mL), dried (Na_2SO_4), and evaporated to dryness. Crystallization from ethyl acetate–*n*-pentane yielded *N*-acetyl-D-*p*-fluorophenylalanine methyl ester in fine colorless needles: yield 1.3 g (87%); mp 90 °C; IR (KBr) ν_{max} 1622 (CONH), 1740 (CO-OCH_3), 3310 (NH) cm^{-1}; ^{1}H NMR ($CDCl_3$) δ 6.8–7.1 (m, 4 H, aromatic), 5.85–6.25 (br, 1 H, NH), 4.6–4.95 (m, 1 H, CH), 3.75 (s, 3 H, $COOCH_3$), 3.0–3.2 (d, 2 H, CH_2), 1.95 (s, 3 H, $NHCOCH_3$); mass spectrum, *m/e* 239; $[\alpha]^{26.5}_D$ −89.6° (*c* 1.55, $CHCl_3$). Anal. Calcd for $C_{12}H_{14}O_3NF$: C, 60.25; H, 5.86; N, 5.86; F, 7.95. Found: C, 60.32; H, 6.04; N, 5.77; F, 8.02.

*N-Acetyl-*L*-p-fluorophenylalanine methyl ester* was prepared by the treatment of diazomethane solution of *N*-acetyl-L-*p*-fluorophenylalanine at 0–5 °C in 91% yield; mp 91 °C. Mixed melting point with the authentic sample of the ester prepared by the method previously described (Gorenstein & Shah, 1982) was unchanged. $[\alpha]^{26.5}_D$ = +88.7° (*c* 1.48, $CHCl_3$).

*N-Acetyl-*D*-p-fluorophenylalaninal* was synthesized by the method previously described (Gorenstein & Shah, 1982) for the preparation of the L enantiomer. $[\alpha]^{26.5}_D$ = −112.2° (*c* 1.42, $CHCl_3$). Anal. Calcd for $C_{11}H_{12}O_2NF$: C, 63.16; H, 5.74; N, 6.70; F, 9.10. Found: C, 62.97; H, 5.92; N, 6.58; F, 9.18.

Methods

^{19}F NMR spectra were recorded on Bruker WP-80 and IBM WP-200 SY spectrometers at 75.26 (^{19}F) and 188.30 MHz (^{19}F), respectively, and ^{1}H NMR spectra on a 60-MHz Varian T-60 spectrometer. Chemical shifts in parts per million for ^{1}H NMR spectra are referenced to external Me_4Si and for ^{19}F NMR spectra are referenced to external CF_3COOH. Mass spectra were taken on an AEI MS-30 spectrometer. Infrared spectra were obtained on a Perkin-Elmer 727B spectrometer. Optical rotations were measured on a Perkin-Elmer 241 polarimeter. Melting points were taken on a Thomas-Hoover apparatus and are uncorrected.

Fluorine NMR Spectra. Cht was dissolved in a 0.1 M phosphate buffer solution in 99.9% D_2O containing 1 mM EDTA, pD = "pH" + 0.4. To this solution was added the aldehyde dissolved in Me_2SO so that the final concentration of Me_2SO was about 20% (v/v) and the aldehyde concentration was about 5 mM (or greater). Enzyme concentrations (2–4 mM) are corrected for active sites, while no correction for enzyme dimerization was made (Gammon et al., 1972). Normally, spectra were obtained without broad-band proton decoupling, with 15 000–20 000 scans, 90° pulses, 2000-Hz sweep width, and 2-s repetition cycle for a Bruker WP-80 spectrometer and with 5000 (no enzyme) or 25 000 scans (with enzyme), 90° pulses, 5000-Hz sweep width, and 1.6-s repetition cycle for an IBM WP-200 SY spectrometer.

Determination of Inhibition Constants (K_i) to Cht. The inhibition constants were determined by standard steady-state kinetics (Dixon & Webb, 1964) against the substrate *N*-benzoyl-L-tyrosine ethyl ester as previously described (Gorenstein & Shah, 1982).

Scheme I

$$RC(O)H \rightleftharpoons RC(OH)_2H$$

$$RC(O)H + Cht \rightleftharpoons RC(O)H \cdot Cht \rightleftharpoons$$

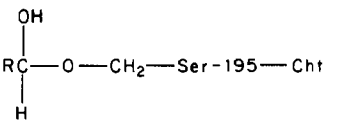

1

Results and Discussion

In most experiments the racemic mixture of the aldehyde was used, although only the L enantiomer is expected to bind especially tightly to the enzyme. Thus, Kennedy & Schultz (1979) have shown that the D enantiomer of BzPheal has a K_i of 1.1 mM while the L enantiomer has a K_i of 0.035 mM (both in 12.5% Me_2SO). In our previous study (Gorenstein & Shah, 1982), we had observed similar differences for the *p*-fluoro aldehyde derivatives. The inhibition constant of the L enantiomer of AcFPheal (0.79 mM) is nearly the same as the inhibition constant of the unfluorinated pure-L derivative (K_i = 0.7 ± 0.2 mM). All aldehydes had previously been shown to behave as competitive inhibitors against *N*-benzoyl-L-tyrosine ethyl ester substrate.

Scheme I best explains previous proton and fluorine NMR studies on the binding of aldehyde transition-state analogues to α-chymotrypsin. Aldehydes readily hydrate in aqueous solution; however, it is the free aldehyde, RC(O)H, and not the hydrate, $RC(OH)_2H$, that is believed to bind to Cht (Chen et al., 1979; Kennedy & Schultz, 1979; Lowe & Nurse, 1977). After initial binding of the aldehyde to Cht to form the noncovalent Michaelis complex, it is converted into the hemiacetal complex, **1**.

The advantage of ^{19}F NMR spectroscopy over ^{1}H NMR or UV–vis spectroscopy is that we can observe separate signals for all the different species shown in Scheme I. Thus in the proton-decoupled ^{19}F NMR spectra of DL-AcFPheal in the absence of Cht, two signals are observed [see Figure 4a of Gorenstein & Shah (1982)] at −37.6 and −38.4 ppm (upfield from an external sample of trifluoroacetic acid standard, D_2O lock). The smaller signal (10% relative area) is assigned to the free aldehyde and the larger signal to the hydrate by analogy to the signal intensities of the two species in the proton NMR spectra (Chen et al., 1979). Because the ^{19}F NMR signal intensity of large macromolecular complexes essentially disappears upon proton decoupling (resulting from a nuclear Overhauser effect, NOE, of −100%; Gerig, 1978; Sykes & Weiner, 1980), most spectra of samples containing enzyme were obtained without proton decoupling. The apparent line width in the proton-coupled spectrum for thee hydrate signal at −38.4 ppm and the free-aldehyde signal at −37.6 ppm is 20–30 Hz, largely due to unresolved ortho and meta proton coupling to the fluorine nucleus.

Upon addition of Cht, two new signals appear at −33.8 (pD 3.8–6) and −36.8 to −37.1 ppm (pD 3.8–9.1) in the proton-coupled ^{19}F NMR spectra (Figure 1). The signal at ca. −36.8 ppm appears as a broad shoulder to the free-aldehyde signal at −37.6 ppm. As discussed earlier in Gorenstein & Shah (1982), assignment of the two new signals to the inhibitor–Cht

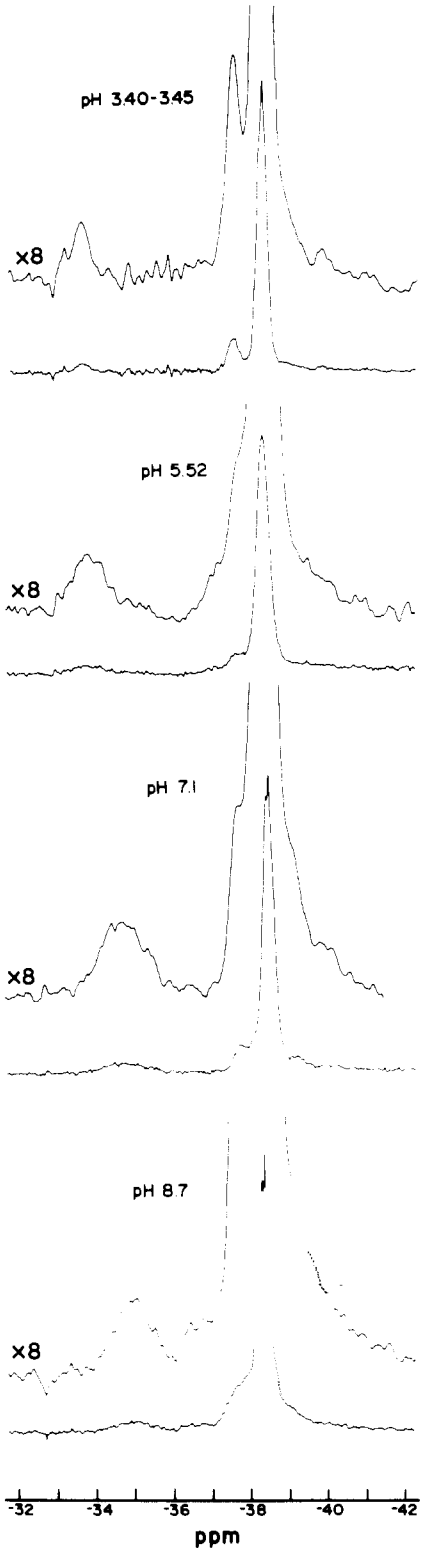

FIGURE 1: ^{19}F NMR spectra of 10 mM DL-AcFPheal in the presence of 2.0 mM α-chymotrypsin at 30 °C: pD 3.8 ± 0.1, 5.9 ± 0.1, 7.5 ± 0.1, and 9.1 ± 0.1 in 20% Me_2SO; no ^1H decoupling; E_0 corrected for 85% active sites. FID exponential multiplication of 2 Hz applied to full-scale spectra and 8 Hz to the expanded spectra.

complex was based upon (1) broader line widths for the enzyme aldehyde signals, (2) signal intensities dependent upon enzyme concentration, and (3) signal disappearance upon decoupling (due to a NOE of −100%).

The −33.8 ppm (pD 3.8–6) signal was assigned to the covalent hemiacetal complex while the −36.8 to −37.1 ppm signal was tentatively assigned to the noncovalent enzyme-bound aldehyde complex (Gorenstein & Shah, 1982). Additional

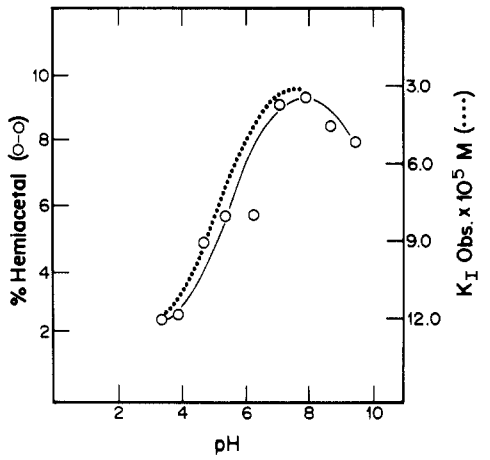

FIGURE 2: Plot of percentage hemiacetal signal intensity at −33.6 ppm (O) for DL-AcFPheal and K_i(obsd) for association of BzPheal to Cht complex (···) as a function of pH at 30 °C: [DL-AcFPheal] was 10 mM and [Cht] was 2 mM.

support for these assignments is now provided by the data shown in Figures 1–5. Note that the chemical shift and signal intensity for the two enzyme-complex signals are pH and temperature dependent. In Figure 2, we plot the percent hemiacetal signal intensity (−33.8 ppm signal) vs. pH. This hemiacetal signal, shifted about 4 ppm downfield (at pH <6) from the other ^{19}F signals, reaches a maximum signal intensity at pH ~8.0 (9.5% total signal area). Actually, since the recycle time in these spectra is 2.0 s and since the T_1 relaxation time is much longer for the small molecules (hydrate or aldehyde) than for any of the enzyme-complex molecules, the hydrate and free-aldehyde signals will be selectively saturated at short recycle times. At very long recycle times, allowing equilibrium magnetization to recover for all signals, the hemiacetal signal area will really be slightly less than the maximum 9.5% [on the basis of Gorenstein & Shah (1982), the maximum hemiacetal signal area would be about 8.5%]. Nevertheless, as before, we note that the ^{19}F signal areas in these spectra will give reliable, relative equilibrium concentrations for the various species.

The approximate 4-fold variation in the hemiacetal signal area as a function of pH is consistent with the similar small variation of K_i over this pH range. Kennedy & Schultz (1979) have also observed that K_i for the association of *N*-benzoyl-L-Pheal to Cht decreases only ~4-fold from pH 3.0 to 8 (see Figure 2, dashed curve). We also find that the *N*-acetyl-DL-Pheal binding constant is 2.5 ± 0.5 mM, 2.2 ± 0.3 mM, and 1.25 ± 0.27 mM at pH 4.0, 5.5, and 7.8, respectively. As discussed by Kennedy & Schultz, this small variation in binding constant with pH is consistent with the binding of the aldehyde as the neutral hemiacetal throughout this pH range. The His-57 imidazole likely functions as in the normal enzymatic mechanism to deprotonate Ser-195 O_γ–H to initially yield the hemiacetal anion. This complex then rapidly picks up a proton to yield the neutral hemiacetal [Scheme II; from Kennedy & Schultz (1979)]. Since the pK of His-57 is ~6.8, it would appear that the neutral hemiacetal is bound slightly more tightly to the protonated His-57 form of the enzyme than to the unprotonated His-57 enzyme (although formation of the hemiacetal could significantly perturb the pK of His-57).

This interpretation gains additional support from the pH dependences of the ^{19}F chemical shifts (Figure 3) and line widths for the hemiacetal–enzyme complex signal. According to Scheme II, the conversion of the initial Michaelis noncovalent complex to the hemiacetal is still going to be catalyzed by His-57 (rate constant k_2, Scheme II). The upfield shift

Scheme II

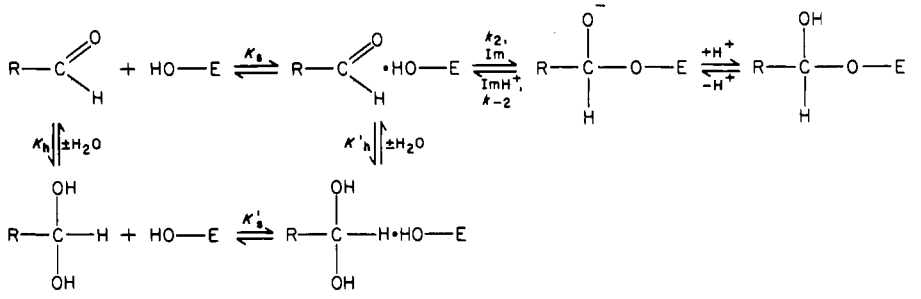

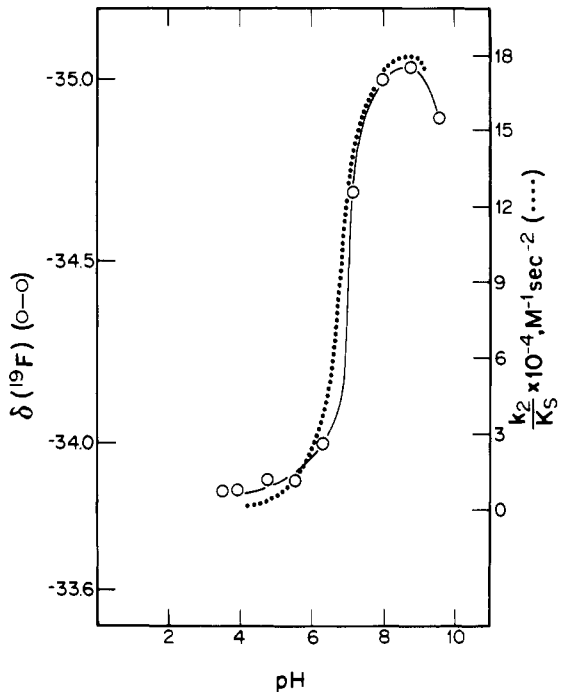

FIGURE 3: Plot of chemical shift δ (^{19}F) (O) of hemiacetal signal for DL-AcFPheal and k_2/K_s (···) for rate of association of BzPheal and *N*-methylhistidine-57–Cht, as a function of pH, at 30 °C: [DL-AcFPheal] was 10 mM and [Cht] was 2 mM.

of the hemiacetal signal from pH 4 to 8 is likely due to an increase in the rate of chemical exchange between the aldehyde and the hemiacetal. Kennedy & Schulz (1979) have shown that k_2/K_s increases with increasing pH between pH 4 and 8 (Figure 3, dashed curve) for the rate of association of *N*-benzoyl-L-Pheal and *N*-methylhistidine-57–Cht. Similar, although faster, rates of association were observed for the native enzyme. It is therefore likely that at low pH (pH <6), the hemiacetal is in slow chemical exchange with the various aldehyde species (free or noncovalent Michaelis complex). Since separate signals are also observed for the free aldehyde and hydrate, these species are also in slow chemical exchange.

As the hemiacetal species more rapidly exchanges with the aldehyde species, the ^{19}F hemiacetal signal will shift in the direction of the aldehyde signals at −37.1 and −37.8 ppm. This is expected as the exchanging system moves from slow to intermediate chemical exchange (Pople et al., 1959). At higher pH (>8.5), the rate of exchange decreases (see k_2/K_s in Figure 3), and the hemiacetal signal begins to shift back to its slow chemical exchange position. Note Cht also has a maximal rate for catalysis of substrates around pH 8 (Blow, 1976).

This explanation for this shift behavior based upon exchange effects is supported by the pH and temperature dependences to the line width of the hemiacetal signal. The line width increases toward a maximum between pH 4 and 8 and then decreases at higher pH (Figure 1). The additional broadening could result from the increased rate of chemical exchange. If one assumes no chemical exchange broadening at pH 4, the additional line broadening at pH 8 is ~50 Hz (110–60 Hz). This chemical exchange broadening component of the line width at pH 8 relates to the rate of chemical exchange $k_{ex} = \pi(\Delta\nu_{1/2})_{ex} \sim 160\ s^{-1}$ (Pople et al., 1959). The additional line broadening with increasing temperature at pH 5.6 (spectra not shown) also suggests that increasing chemical exchange, and hence, line broadening, occurs at higher temperature as the system moves from slow to intermediate chemical exchange. According to Kennedy & Schultz, the rate constant k_3 for conversion of the Cht Michaelis complex to hemiacetal for *N*-benzoyl-L-Pheal is estimated to be $8.0 \times 10^4\ s^{-1}$, while the back-reaction rate constant, k_{-2}, is $42\ s^{-1}$. Since *N*-benzoyl-L-Pheal binds tighter than *N*-acetyl-L-Pheal (Chen et al., 1979), k_{-2} for the later inhibitor is probably faster and in reasonable agreement with the NMR estimate for exchange. Our determination of K_{eq} ($=k_2/k_{-2}$) based upon the signal intensities for the Michaelis complex and the hemiacetal, which are roughly equal (see below), suggests that k_2 and k_{-2} for Ac-Pheal are also roughly equal. In contrast, no ^{19}F NMR signal for the Michaelis complex in the association of *N*-benzoyl-DL-FPheal with Cht has been observed (Gorenstein & Shah, 1982), consistent with the kinetically determined equilibrium constant of Kennedy & Schultz, which favors hemiacetal formation for this inhibitor.

^{19}F NMR Spectra at High Field. Better resolution of the different ^{19}F signals is achieved at 188.3 MHz (^{19}F) (Figure 4). The noncovalent Michaelis complex signal at −37.1 ppm (Figure 4A–C) is now well separated from the free-aldehyde signal at −37.6 ppm.

The ratio of the hemiacetal complex signal at −33.7 ppm to the Michaelis complex signal at −37.1 ppm is 0.86, 3.0, and 1.8 at pD 4.1, 7.0, and 8.5, respectively. This 3–4-fold variation with pH in the equilibrium ratio of the covalent to noncovalent enzyme complexes parallels nicely the 4-fold variation with pH in the percent hemiacetal and inhibition constant discussed earlier (Figure 2). At lower pH, more of the inhibitor is noncovalently bound, which explains why the inhibitor binds less tightly at low pH. The decrease in the percent hemiacetal signal in alkaline pH (Figure 2) is also apparently due to a shift in the equilibrium toward the noncovalent complex.

Several additional signals can also be observed at high field. Small upfield signals at −39.1 and −40.0 ppm integrating for less than 1% of the total signal area are possibly due to other binding geometries for the inhibitor complex or simply impurities in the aldehyde preparation. Indeed, as shown in the fully decoupled spectrum (Figure 4D) of the aldehyde with no added enzyme, some weak additional signals of less than 1% intensity appear to be present (the same lot of aldehyde was used in the preparation of all four samples of Figure 4). Additional signals near the free-aldehyde signal are probably associated with the D enantiomer (see below).

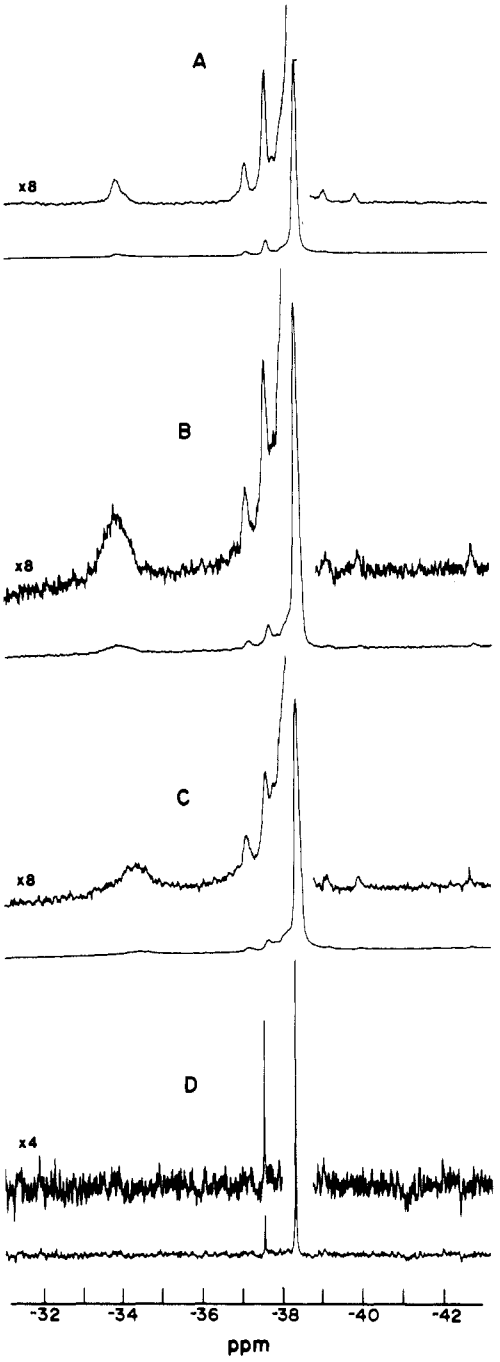

FIGURE 4: ^{19}F NMR spectra on an IBM WP-200 SY spectrometer of DL-AcFPheal in the presence of Cht at 30 °C in 20% Me_2SO: no ^1H decoupling except for (d); E_0 corrected for 85% active sites. (a) 10 mM DL-aldehyde, 2 mM Cht, pD 4.1; (b) 5 mM DL-aldehyde, 2 mM Cht, pD 7.0; (c) 10 mM DL-aldehyde, 2 mM Cht, pD 8.5; (d) 20 mM DL-aldehyde, no Cht, pD 6.0 with broad-band proton decoupling.

^{19}F NMR Spectra of Resolved Aldehyde–Cht Complexes. The above peak asssignments, based upon spectra of the DL racemate, are fully supported by separate spectra of Cht with the resolved enantiomers of AcFPheal. As shown in Figure 5, only the more tightly bound L-aldehyde appears to form the hemiacetal complex. The maximum amount of the hemiacetal species at pH ~6.0 under high E_0/I_0 ratio for DL-AcFPheal was 6% (Gorenstein & Shah, 1982). Under the same conditions for the pure L enantiomer, the maximum amount of the hemiacetal is 12% (Figure 5A). The D enantiomer in the racemic mixture thus does not contribute to the hemiacetal signal area. A very small (<1% total signal area) signal is barely observed at −33.8 ppm in the D-aldehyde spectrum

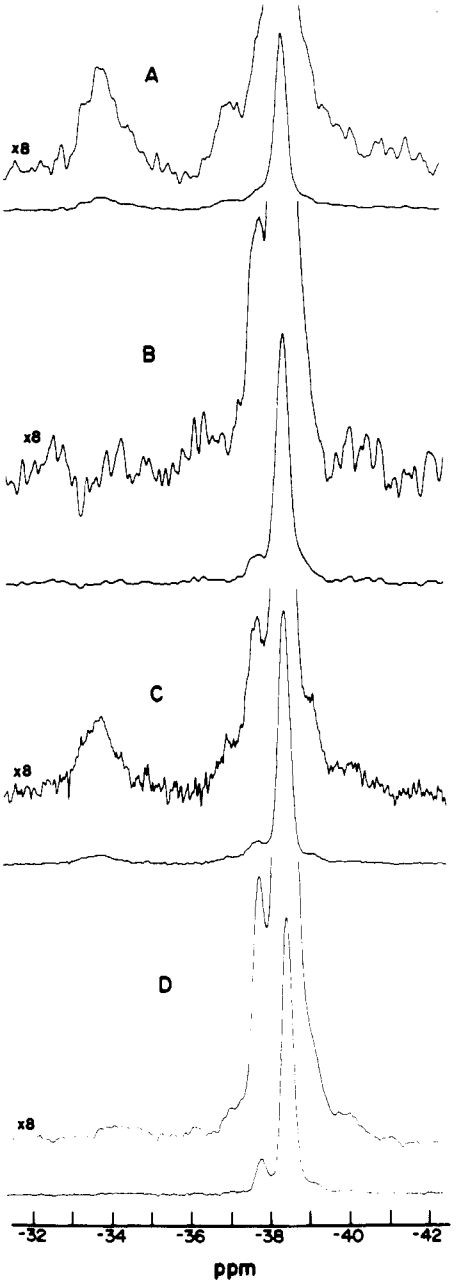

FIGURE 5: ^{19}F NMR spectra of the D as well as the L isomer of AcFPheal in the presence of Cht at 30 °C and pD 6.0 ± 0.1 in 20% Me_2SO: no ^1H decoupling; E_0 corrected for 85% active sites. (a) 5 mM L-aldehyde, 2.0 mM Cht; (b) 5 mM D-aldehyde, 2.0 mM Cht; (c) 20 mM L-aldehyde, 4.0 mM Cht; (d) 20 mM D-aldehyde, 4.0 mM Cht. FID exponential multiplication of 8 Hz applied to (a) and (b), 2 Hz to (c), and 2 Hz to lower spectrum and 8 Hz to enlarged spectrum shown above in (d).

(Figure 5B). This signal is almost below detection, however, and is attributed to a small contaminating amount of L-aldehyde in the D-aldehyde sample. We have found that the optically pure D-AcFPheal undergoes slow epimerization ($\tau_{1/2}$ ~ 18 h) at pH 8.0, 31 °C, as measured by the loss in optical rotation over time. Since many of the ^{19}F NMR spectra require signal averaging overnight, a significant amount of epimeration occurs, especially at higher pH. In fact, at pH 8.3, the ^{19}F NMR spectra for the "D" enantiomer appears quite similar to the "L" enantiomer except for the relative intensity of the hemiacetal signal (spectra not shown). All of this intensity is attributable to partial epimerization of the sample.

Only a small signal assignable to a noncovalent Michaelis complex at −37.1 to −36.8 ppm can be observed for the bound

D-aldehyde. This suggests that the D enantiomer cannot form the hemiacetal complex. Indeed, if the aromatic side chain of the D enantiomer is placed in the hydrophobic-specificity pocket and the α-H is the only group sterically able to fit the α-H-specificity locus, then the α-C(O)H group must be placed into the *N*-acylamino binding pocket and the *N*-acylamino group placed into the catalytic locus proximate to O_γ of Ser-195 (Gammon et al., 1972). With this binding arrangement, the D-aldehyde is incapable of forming the hemiacetal since the aldehyde carbon is too far from the O_γ of Ser-195.

Registry No. Cht, 9004-07-3; DL-AcFPheal, 82657-49-6; L-AcFPheal, 82691-34-7; D-AcFPheal, 87638-54-8; L-AcFPhe, 330-81-4; D-AcFPhe methyl ester, 87586-95-6; L-AcFPhe methyl ester, 87586-96-7; DL-AcFPhe methyl ester, 87586-97-8; L-AcPheal, 35593-55-6.

References

Aoyagi, T., Miyata, S., Nanbo, M., Kojima, F., Matsuzaki, M., Ishizuka, M., Takeuchi, T., & Umezawa, H. (1969) *J. Antibiot. 22*, 558.

Blow, D. (1976) *Acc. Chem. Res. 9*, 145.

Breaux, E. J., & Bender, M. L. (1975) *FEBS Lett. 56*, 81.

Chen, R., Gorenstein, D. G., Kennedy, W. P., Lowe, G., Nurse, D., & Schultz, R. M. (1979) *Biochemistry 18*, 921.

Clark, P. I., Lowe, G., & Nurse, D. (1977) *J. Chem. Soc., Chem. Commun.*, 451.

Dixon, M., & Webb, E. C. (1964) *Enzymes*, 2nd ed., p 327, Academic Press, New York.

Gammon, K. L., Smallcombe, S. H., & Richards, J. H. (1972) *J. Am. Chem. Soc. 94*, 4573.

Gerig, J. T. (1978) in *Biochemical Magnetic Resonance* (Berliner, L. J., & Reuben, J., Eds.) Chapter 5, Plenum Press, New York.

Gorenstein, D. G., & Shah, D. O. (1982) *Biochemistry 21*, 4679.

Gorenstein, D. G., Kar, D., & Momii, R. K. (1976) *Biochem. Biophys. Res. Commun. 73*, 105.

Ito, A., Tokawa, K., & Shimizu, B. (1972) *Biochem. Biophys. Res. Commun. 49*, 343.

Ito, A., Tamahashi, R., & Baba, Y. (1975) *Chem. Pharm. Bull. 23*, 3081.

Kawamura, K., Kondo, S., Maeda, K., & Umezawa, H. (1969) *Chem. Pharm. Bull. 17*, 1902.

Kennedy, W. P., & Schultz, R. M. (1979) *Biochemistry 18*, 349.

Kondo, S., Kawamura, K., Iwanaga, J., Hanada, M., Aoyagi, T., Maeda, K., Takeuchi, T., & Umezawa, H. (1969) *Chem. Pharm. Bull. 17*, 1896.

Lienhard, G. E. (1972) *Annu. Rep. Med. Chem. 7*, 249.

Lienhard, G. E. (1973) *Science (Washington, D.C.) 180*, 149.

Lowe, G., & Nurse, D. (1977) *J. Chem. Soc., Chem. Commun.*, 815.

Pauling, L. (1946) *Chem. Eng. News 24*, 1375.

Pople, J., Schneider, W. G., & Bernstein, H. J. (1959) *High Resolution Nuclear Magnetic Resonance*, McGraw-Hill, New York.

Schonbaum, G. R., Zerner, B., & Bender, M. L. (1961) *J. Biol. Chem. 236*, 2930.

Schultz, R. M., & Cheerva, A. C. (1975) *FEBS Lett. 50*, 47.

Sykes, B. D., & Weiner, J. H. (1980) *Magn. Reson. Biol. 1*, 171–196.

Thompson, R. C. (1973) *Biochemistry 12*, 47.

Thompson, R. C. (1974) *Biochemistry 13*, 5495.

Wolfenden, R. (1972) *Acc. Chem. Res. 5*, 10.

Wyeth, P., Sharma, R. P., & Akhtar, M. (1980) *Eur. J. Biochem. 105*, 581.

Deuterium Nuclear Magnetic Resonance Study of the Effects of Palmitic Acid on Dipalmitoylphosphatidylcholine Bilayers†

K. Peter Pauls,* Alex L. MacKay, and Myer Bloom

ABSTRACT: The physical effects of 20 mol % palmitic acid on bilayers of dipalmitoylphosphatidylcholine were examined by deuterium nuclear magnetic resonance, and the fidelity of deuterated fatty acids as membrane probes was examined by comparing samples in which either the free fatty acid or the fatty acyl chains of the phospholipid were perdeuterated. Addition of palmitic acid increased the temperature of the phase transition onset by 2 °C and broadened the coexistence region of gel and liquid-crystalline lipid to span 7–10 °C, depending on which sample was examined. Average order parameters for samples containing free fatty acid were approximately 10% higher than those observed for pure DPPC. Order parameter profiles estimated by an empirical method indicated that the ordering effect of palmitic acid was felt down the whole length of the phospholipid acyl chains. Measurements of the quadrupolar echo relaxation rate suggested that addition of fatty acid inhibits slow motions of the phospholipid side chains. In general, the results indicate that free fatty acid probes perturb the structure of membranes into which they are incorporated but that they are accurate reporters of the order in the perturbed system.

Free fatty acids occur as components of biological membranes, albeit in small quantities (Ray et al., 1969; Mead & Mertin, 1978). Exogenous additions of free fatty acids have been shown to alter a variety of membrane-mediated cellular functions including membrane-bound enzyme activity (Orly & Schramm, 1975; Glass et al., 1977; Rhoads et al., 1982; Schmalzing & Kutschera, 1982), platelet aggregation (Hoak et al., 1970), cell permeability (Shramm et al., 1967), cell fusion (Ahkong et al., 1973; Kantor & Prestegard, 1975), and lymphocyte mitogenesis (Mead & Mertin, 1978). Some of these effects are thought to be the result of fatty acid induced changes in membrane structure.

† From the Department of Physics, University of British Columbia, Vancouver, British Columbia, Canada V6T 1W5. *Received May 16, 1983.* This research was supported by the Natural Sciences and Engineering Research Council of Canada.

* Address correspondence to this author at the Department of Crop Science, University of Guelph, Guelph, Ontario, Canada N1G 2W1.

0006-2960/83/0422-6101$01.50/0